Hindawi
Wireless Communications and Mobile Computing
Volume 2020, Article ID 8886487, 13 pages
https://doi.org/10.1155/2020/8886487

Research Article

Outage Probability Analysis of Decode-and-Forward Two-Way Relaying System with Energy Harvesting Relay

Hoang Van Toan,[1] Tran Manh Hoang,[1] and Le The Dung[2,3]

[1]*Telecommunications University, Khanh Hoa Province, Vietnam*
[2]*Division of Computational Physics, Institute for Computational Science, Ton Duc Thang University, Ho Chi Minh City, Vietnam*
[3]*Faculty of Electrical and Electronics Engineering, Ton Duc Thang University, Ho Chi Minh City, Vietnam*

Correspondence should be addressed to Le The Dung; lethedung@tdtu.edu.vn

Received 23 April 2020; Revised 29 October 2020; Accepted 22 November 2020; Published 7 December 2020

Academic Editor: Hideyuki Takahashi

In this paper, we evaluate a two-way relay system consisting of two terminals and an intermediate relay. In this model, two terminals do not have a direct link but exchange data with each other via the relay in three phases. The relay utilizes energy harvesting technology to collect energy from the received signals of two terminals in the first two phases and then uses the obtained energy for signal transmission in the third phase. Each node is equipped with a single antenna and operates under a half-duplex mode. All wireless channels are influenced by reversible independent flat Rayleigh fading. Using analytical methods, we provide the exact and approximate closed-form expressions of user outage probability and system outage probability. The approximate expressions of these outage probabilities are more explicit and straightforward, providing a better understanding of the influences of network parameters on the system quality. Monte-Carlo simulations are used to confirm the correctness of mathematical analyses.

1. Introduction

Nowadays, energy harvesting (EH) technology has become a hot research trend and attracted increasing interest from many research groups around the world [1–3]. It is a research trend towards green information in which network nodes can harvest the energy from different sources, such as solar, wind, vibration, thermoelectric effects, and other physical phenomena [4–6]. Based on the fact that radio frequency (RF) signals can carry energy and information at the same time [7], a new emerging solution for a wireless network is to avail ambient RF signals, in which wireless nodes can harvest energy and process the information simultaneously. Therefore, with EH technology, network nodes can collect energy from received signals in the radio band and use it for next operations [8, 9]. This operation not only helps to extend the operation life time of wireless nodes but also reduces their battery usage, resulting in a reduction of toxic wastage. Generally, based on the operation of receiver, EH technology is divided into two main techniques: (i) time switching (TS), where the received signal is divided into two time phases to harvest energy and decode the signal, and (ii) power splitting (PS), where the received signal power is split into two parts for energy harvesting and signal decoding [9]. Based on receiver architecture, EH systems are divided into two main categories: (i) harvest-use, where all harvested energy is used immediately, and (ii) harvest-store-use, where harvested energy can be stored for the next operation [10]. For the receiver applying the TS scheme, its antenna is successively connected to the energy harvesting block and the signal processing block. The timing mechanism controls the signals coming to these blocks. On the contrary, for the receiver using the PS scheme, its antenna is connected to both the energy harvesting block and data processing block; thus, the received data are shared between them. Therefore, the EH phase and the information processing phase may concurrently occur in a given time slot, which shortens the transmission cycle. However, from the receiver's complexity perspective, the TS scheme is superior to the PS scheme because the commercially available circuits

separately designed for information decoding and energy harvesting can be used [11–13].

Recently, two-way relay systems have also been received much attention from researchers as they can improve spectral efficiency and extend the coverage area of wireless communication systems [14–17]. In [14], the authors study a system model where a bidirectional connection between two terminals is established via one amplify-and-forward (AF) or decode-and-forward (DF) relay and propose a novel relaying protocol where two relays alternately forward messages from a source terminal to a destination terminal, namely, two-path relaying. In [15], a two-way amplify-forward communication system employing the EH technique at relay node over Nakagami-m fading channels was considered. The authors gave the exact closed-form expression of user outage probability, the approximated expression of system outage probability, and the upper bound of ergodic capacity. The authors in [16] derived the expression of system outage probability and the sum-rate of a two-way network where two users exchanging information via multiple AF relays. To study the performance of a single relay selection scheme in a two-way relay system under outdated CSI conditions, the authors in [17] provided the exact and asymptotic expressions of the system outage probability. Similar to other systems, wireless nodes in two-way relay systems also encounter the problem of saving energy to extend the communication time. Therefore, the idea of combining EH technology in two-way systems is a new solution and has been studied in a number of recent publications. In [18], the authors considered a two-way relay cognitive radio system with a primary receiver. They evaluated this decode-and-forward (DF) relay system where the relay applies EH technology and network coding by deriving a closed-form expression of the system outage probability at terminals. However, this probability expression was not explicitly given. In [19], the authors studied the maximum throughput of a two-way relay system where two terminals and relay use EH technology. An energy harvesting two-way dual-relay network consisting of one non-EH relay and one EH relay with a finite-sized battery was investigated in [20]. The authors in [21] analyzed the outage probability and throughput of a three-phase two-way DF relay system model where the relay harvests the energy from radio frequency signals in the first two phases and converts it to transmission power in the third phase. However, in [21], the closed-form expression of overall system outage probability was not given. In [22], the authors considered three-step two-way decode-and-forward (DF) relay networks which are similar to the system model considered in [21]. Although they derived an analytical expression for the system outage probability and proposed a dynamic power splitting (PS) scheme to minimize the system outage probability, similar to [21], the exact expression of system outage probability was not given and the derivations of approximate expression are very complex and difficult to follow. The authors in [23] studied a two-way relaying system consisting of a multiantenna relay and two single-antenna sources. The relay was not properly powered but had to collect the energy from two sources' transmitted signals in the broadcast phase. Two sources exchanged information in two time phases. The system performance in terms of outage probability and average throughput was analyzed. However, because the SNR expression was too complicated, they could not give closed-form expressions of these performance metrics. In [24], the authors consider relay beamforming and power-domain nonorthogonal multiple access for a wireless-powered multipair two-way relay network. Their objective was to optimize the energy transfer beamforming matrix by maximizing the minimum of the achievable rates among all the users. Applying a piecewise linear energy harvesting model for the users and the relay in dual-hop wireless powered two-way communication, the authors in [25] investigated the problem of total throughput maximization of both AF and DF relaying models. They concluded that it is essential to study a realistic EH model as the impractical linear EH model causes tremendous performance loss.

Motivated by the above issues, in this paper, we will derive the exact and approximate closed-form expression of overall system outage probability using the Taylor series expansion and Gaussian-Chebyshev quadrature approach. The approximation expressions are presented in a more concise form, allowing us to see the effects of key parameters such as the average transmission power, the channel gain, the time allocation of signal phase, and the power allocation coefficient on the system outage performance more easily. Particularly in this paper, the time allocation ratio of the signal phase and the power allocation coefficient are the distinguished parameters of the considered two-way DF relay system with EH relay; thus, it is necessary to clarify these parameters' influences on the outage performance of the considered system. Moreover, using the Taylor series expansion and Gaussian-Chebyshev quadrature approach allows us to adjust necessary precision by changing the number of terms in finite sum.

The rest of this paper is organized as follows. Section 2 outlines the proposed system model. The outage probability of this system model is studied in Section 3. Section 4 presents numerical results. Section 5 concludes the main findings of this paper.

2. System Model

In this paper, we consider a two-way relay system as shown in Figure 1. This system comprises two terminals S_1 and S_2 exchanging their data via an intermediate relay node R. The relay R is assumed to have a limited power and therefore has to harvest the energy from the radio frequency signals of two terminals to forward the information of these two terminals by using the DF three-phase two-way relay protocol. The motivation for using the DF relay are as follows: (i) the DF relay is found to be of more practical interest; (ii) compared with the AF relaying strategy, DF relaying avoids noise amplification and can be easily combined with coding technologies. All wireless channels are assumed to be reciprocal and undergo independent flat Rayleigh fading.

The three-phase two-way relay protocol can be described as follows. A cycle T for signal transmission between two terminals is divided into three phases. In the first phase t_1, after

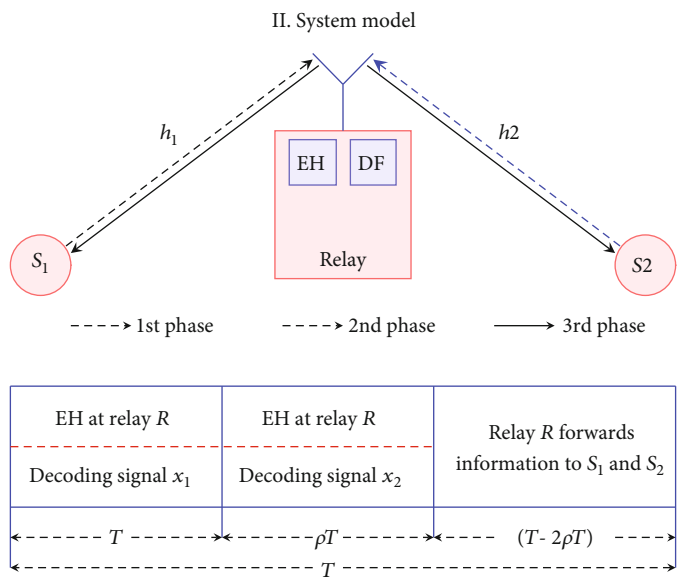

Figure 1: System model of the two-way DF relay system with EH relay.

R receives signals from S_1, a power divider is used to divide the received power into two parts: one part is used to process signal and another part is used to convert energy. In the second phase t_2, S_2 transmits its signal to R. Then, R divides the power of the received signal similarly to the first phase. It is assumed that $t_1 = t_2 = \rho T$, where $0 < \rho < 0.5$ is the time allocation ratio of the signal phase. In the third phase $t_3 = (1 - 2\rho)T$, the relay broadcasts the reencoding signals to two terminals.

We assume that the global channel state information (CSI) and partial CSI for the relay and terminals can be acquired perfectly. Specifically, for the relay R, the CSI of h_1 and h_2 have to be acquired to correctly decode the signal from two users simultaneously. For the terminal S_1 (S_2), the CSI of h_1 (h_2) have to be acquired to correctly decode the desired signals. In our considered relay system, the channel coefficients h_1 and h_2 can be obtained as follows. Terminal S_1 broadcasts a ready-to-send (RTS) message before information transmission. After receiving the RTS message from S_1, terminal S_2 replies with a clear-to-send (CTS) message. Then, the relay R can estimate the channel coefficients of both h_1 and h_2 by overhearing the RTS and CTS messages. Finally, terminals S_1 and S_2 are informed of the corresponding channel coefficients through the feedbacks from the relay R [26].

Denote h_i, $i \in \{1, 2\}$, as the channel coefficients between S_i and R. When S_i transmits with power P, the received signal at R in the ith phase is

$$y_{\mathrm{R}}^{i} = \sqrt{P} h_i x_i + n_i, \tag{1}$$

where n_i is an additive white Gaussian noise at the relay in the ith phase time, x_i is the transmitted signal symbol from S_i, and $\mathbb{E}\{x_i^2\} = 1$.

In the first two phases, R uses the divider to divide the received signal power into two parts: $\sqrt{\delta} y_R^i$ to harvest energy and $\sqrt{1-\delta} y_R^i$ to signal processing, where δ is the power allocation coefficient, $0 < \delta < 1$. The received power at R from S_i is given by

$$E_i = \eta \delta P |h_i|^2 \rho T, \tag{2}$$

where η is the energy conversion efficiency, $0 < \eta < 1$.

Consequently, we have the total energy which the relay collects in two phases as

$$E_{\sum\boxtimes} = \eta \delta P \rho T \left(|h_1|^2 + |h_2|^2\right). \tag{3}$$

It is worth noticing that the receiver consumes a certain amount of energy for CSI acquisition and circuitry. However, in our considered relay system, we assume the power required for CSI acquisition and circuitry is not supplied by the harvester energy but from an independent battery [10]. Thus, when all energy harvested in two phases is used for the signal transmission power of R in the third phase, the transmission power of R in the third phase is

$$P_R = \eta \delta P \left(\frac{\rho}{1 - 2\rho}\right) \left(|h_1|^2 + |h_2|^2\right). \tag{4}$$

According to the DF relaying protocol, R receives signals from S_1 and S_2 in two phases and decodes the received signals y_R^1 and y_R^2 into symbols x_1 and x_2, respectively. Then, R encodes these two decoded symbols by applying XOR operation and obtains the normalized symbol x_R, i.e., $x_1 \oplus x_2 \rightarrow x_R$, where $\mathbb{E}\{x_R^2\} = 1$ and $\oplus$ is the bitwise XOR operation.

In the third phase, R broadcast x_{R} to S_1 and S_2. Terminal S_i receives this symbol and decodes it by using XOR operation with its transmitted symbol. Consequently, the received

signal at S_i in the third phase is given by

$$y_{S_i} = \sqrt{P_R} h_i x_R + n_{S_i}, \tag{5}$$

where n_{S_i} is the AWGN at S_i.

Since the noise power at all nodes in the system is equal to N_0, the signal-to-noise ratios (SNRs) at R in the first and second phases are, respectively, calculated as

$$\gamma_1 = \frac{P(1-\delta)|h_1|^2}{N_0}, \tag{6}$$

$$\gamma_2 = \frac{P(1-\delta)|h_2|^2}{N_0}. \tag{7}$$

In the third phase, the SNR of the received signal at S_i, $i \in \{1, 2\}$, can be calculated as

$$\gamma_{3i} = \frac{\eta\delta P(\rho/(1-2\rho))\left(|h_1|^2 + |h_2|^2\right)|h_i|^2}{N_0}. \tag{8}$$

3. Performance Analysis

3.1. User Outage Probability (UOP)

3.1.1. Exact Expression. In the three-phase two-way relay protocol, the user outage probability of terminal S_i is the probability that S_i cannot successfully decode the intended received signal from S_j. In other words, the user outage probability of S_i is the probability that the SNR of the received signal at S_i is less than a threshold γ_{th}, i.e.,

$$\text{UOP}_i = \Pr\left(\gamma_{ji} < \gamma_{\text{th}}\right), \tag{9}$$

where $\gamma_{ji} = \min(\gamma_j, \gamma_{3i})$ with $i, j \in \{1, 2\}, i \neq j$ and $\gamma_{\text{th}} = 2^{3\mathscr{R}} - 1$; $\mathscr{R}$ is the desired data transfer rate of S_i.

We can rewrite (9) as

$$\begin{aligned}\text{UOP}_i &= \Pr\left(\min\left(\gamma_j, \gamma_{3i}\right) < \gamma_{\text{th}}\right) = 1 - \Pr\left(\min\left(\gamma_j, \gamma_{3i}\right) > \gamma_{\text{th}}\right) \\ &= 1 - \Pr\left(\gamma_j > \gamma_{\text{th}}, \gamma_{3i} > \gamma_{\text{th}}\right) = 1 - \Pr\left(\frac{P(1-\delta)|h_j|^2}{N_0} > \gamma_{\text{th}}, \eta\delta P \right. \\ &\quad \left. \cdot \left(\frac{\rho}{1-2\rho}\right)\frac{\left(|h_i|^2 + |h_j|^2\right)|h_i|^2}{N_0} > \gamma_{\text{th}}\right).\end{aligned} \tag{10}$$

For clarity, we set $X = |h_i|^2$, $Y = |h_j|^2$, $\phi = \eta\delta\rho/(1-2\rho)$. Then, X and Y are exponential distributed random variables with mean parameters λ_x and λ_y, respectively. Hence, the UOP of S_i is computed as

$$\text{UOP}_i = 1 - \Pr\left(Y > \frac{\gamma_{\text{th}} N_0}{P(1-\delta)}, Y > \frac{\gamma_{\text{th}} N_0}{\phi P X} - X\right). \tag{11}$$

More specifically, the user outage probability at the terminal node S_i is defined in the following Theorem 1.

Theorem 1. *The user outage probability of S_i in the considered two-way DF communication system with EH relay is given by*

$$\begin{aligned}UOP_i &= 1 - e^{-\left((x_0/\lambda_x) + \left(\gamma_{th} N_0/P(1-\delta)\lambda_y\right)\right)} \\ &\quad - \frac{1}{\lambda_x}\sum_{n=0}^{N} \boxtimes \frac{(-1)^n}{n!}\left(\frac{1}{\lambda_x} - \frac{1}{\lambda_y}\right)^n \left(\frac{\gamma_{th} N_0}{\phi P \lambda_y}\right)^{n/2} x_0^{(n+2)/2} e \\ &\quad -\left(\gamma_{th} N_0/2\phi P \lambda_y x_0\right) W_{(-n-2)/2,(n+1)/2}\left(\frac{\gamma_{th} N_0}{\phi P \lambda_y x_0}\right),\end{aligned} \tag{12}$$

where $x_0 = -(\gamma_{th} N_0/2P(1-\delta)) + (\sqrt{\gamma_{th} N_0}\sqrt{4P(1-\delta)^2 + \gamma_{th} N_0 \phi}/2P(1-\delta)\sqrt{\phi})$, $W_{\alpha,\beta}(\cdot)$ *denotes the function Whittaker ([27], Eq. (9.220)), and N is the number of truncated terms in the series expansion.*

Proof. See Appendix A.

3.1.2. Approximate Expression in High SNR Regime. Herein, we use the Gaussian-Chebyshev quadrature approach to calculate the integral of a given function over interval (a, b) as

$$\int_a^b \boxtimes f(x)dx \approx \frac{b-a}{2}\sum_{v=1}^{V} \boxtimes \omega_V \sqrt{1-y_v^2} f(x_v), \tag{13}$$

where $x_v = ((b-a)/2)y_v + (b+a)/2$, $y_v = \cos(((2v-1)/2V)\pi)$, and $\omega_V = \pi/V$.

Then, the approximate value of I_{1a} in (A.5) is

$$\tilde{I}_{1a} \approx \frac{1}{\lambda_x}\sum_{n=0}^{N} \boxtimes \frac{(-1)^n}{n!}\left(\frac{1}{\lambda_x} - \frac{1}{\lambda_y}\right)^n \frac{x_0}{2}\sum_{l=1}^{L} \boxtimes \omega_L \sqrt{1-y_l^2} x_l^n e^{-\left(\gamma_{th} N_0/\phi P \lambda_y x_l\right)}, \tag{14}$$

where $y_l = \cos(((2l-1)/2L)\pi)$, $\omega_L = \pi/L$, $x_l = x_0/2(y_l + 1)$, and L is a parameter that determines the tradeoff between complexity and accuracy.

Finally, the approximate expression of the UOP of S_i is determined in the following corollary.

Corollary 2. *The approximate expression of the UOP of S_i is given by*

$$\begin{aligned}UOP_i^{P\to\infty} &\approx 1 - e^{-\left((x_0/\lambda_x) + \left(N_0/P(1-\delta)\lambda_y\right)\gamma_{th}\right)} \\ &\quad - \frac{1}{\lambda_x}\sum_{n=0}^{N} \boxtimes \frac{(-1)^n}{n!}\left(\frac{1}{\lambda_x} - \frac{1}{\lambda_y}\right)^n \frac{x_0}{2}\sum_{l=1}^{L} \boxtimes \omega_L \sqrt{1-y_l^2} x_l^n e^{-\left(\gamma_{th} N_0/\phi P \lambda_y x_l\right)}.\end{aligned} \tag{15}$$

Thanks to a more straightforward form than in (12), we can easily see the impacts of system parameters on each terminal's outage probability.

3.2. System Outage Probability (SOP)

3.2.1. Exact Expression. The outage probability of a two-way relay system is the probability that the SNR in at least one phase is lower than a given threshold γ_{th}.

Denote $\gamma_e = \min(\gamma_{3i}, \gamma_{3j})$, the system outage probability is calculated as

$$\text{SOP} = 1 - \Pr\left(\gamma_i > \gamma_{\text{th}}, \gamma_j > \gamma_{\text{th}}, \gamma_e > \gamma_{\text{th}}\right) = 1 - I_2 - I_3, \quad (16)$$

where

$$I_2 = \Pr\left(\gamma_i > \gamma_{\text{th}}, \gamma_j > \gamma_{\text{th}}, \gamma_e > \gamma_{\text{th}}, |h_j|^2 > |h_i|^2\right), \quad (17)$$

$$I_3 = \Pr\left(\gamma_i > \gamma_{\text{th}}, \gamma_j > \gamma_{\text{th}}, \gamma_e > \gamma_{\text{th}}, |h_i|^2 > |h_j|^2\right). \quad (18)$$

Then, the system outage probability of the considered system is defined in the following Theorem 3.

Theorem 3. *The exact closed-form expression of the system outage probability of the considered two-way DF relay system with EH relay is given by*

$$SOP = 1 - \exp\left(-\frac{\gamma_{th}N_0}{P(1-\delta)}\left(\frac{1}{\lambda_x} + \frac{1}{\lambda_y}\right)\right) when \frac{P < 2\phi\gamma_{th}N_0}{(1-\delta)^2}, \quad (19)$$

$$\begin{aligned} SOP = {} & 1 - e^{-\left((1/\lambda_x)+(1/\lambda_y)\right)\sqrt{\gamma_{th}N_0/2\phi P}} \\ & - \frac{1}{\lambda_x}\sum_{n=0}^{N} \boxtimes \frac{(-1)^n}{n!}\left(\frac{1}{\lambda_x} - \frac{1}{\lambda_y}\right)^n \left(\frac{\gamma_{th}N_0}{\phi P\lambda_y}\right)^{n/2} \\ & \cdot \left(\begin{array}{l} x_1^{(n+2)/2} e^{-\left(\gamma_{th}N_0/2\lambda_y\phi P x_1\right)} W_{(-n-2)/2,(n+1)/2}\left(\frac{\gamma_{th}N_0}{\lambda_y\phi P x_1}\right) \\ -\left(\frac{\gamma_{th}N_0}{P(1-\delta)}\right)^{(n+2)/2} e^{-\left((1-\delta)/(2\lambda_y\phi)\right)} W_{(-n-2)/2,(n+1)/2}\left(\frac{1-\delta}{\lambda_y\phi}\right) \end{array} \right) \\ & - \frac{1}{\lambda_y}\sum_{n=0}^{N} \boxtimes \frac{(-1)^n}{n!}\left(\frac{1}{\lambda_y} - \frac{1}{\lambda_x}\right)^n \left(\frac{\gamma_{th}N_0}{\phi P\lambda_x}\right)^{n/2} \\ & \cdot \left(\begin{array}{l} x_1^{(n+2)/2} e^{-\left(\gamma_{th}N_0/2\lambda_x\phi P x_1\right)} W_{(-n-2)/2,(n+1)/2}\left(\frac{\gamma_{th}N_0}{\lambda_x\phi P x_1}\right) \\ -\left(\frac{\gamma_{th}N_0}{P(1-\delta)}\right)^{n+2/2} e^{-\left((1-\delta)/2\lambda_x\phi\right)} W_{(-n-2)/2,(n+1)/2}\left(\frac{1-\delta}{\lambda_x\phi}\right) \end{array} \right) when \frac{P > 2\phi\gamma_{th}N_0}{(1-\delta)^2}, \end{aligned} \quad (20)$$

where $x_1 = \sqrt{\gamma_{th}N_0/(2\phi P)}$.

Proof. See Appendix B.

In summary, depending on the transmission power P, the SOP is determined by (19) when $P < 2\phi\gamma_{\text{th}}N_0/(1-\delta)^2$ or by (20) when $P > 2\phi\gamma_{\text{th}}N_0/(1-\delta)^2$.

3.2.2. Approximate Expression in High SNR Regime. Recalling the Gaussian-Chebyshev quadrature approach in (13), the approximate value of I_{2a} in (B.7) is as

$$\tilde{I}_{2a} \approx \frac{1}{\lambda_x}\sum_{n=0}^{N} \boxtimes \frac{(-1)^n}{n!}\left(\frac{1}{\lambda_x} - \frac{1}{\lambda_y}\right)^n \frac{1}{2}\left(x_1 - \frac{\gamma_{\text{th}}N_0}{P(1-\delta)}\right)\sum_{k=1}^{K} \boxtimes \omega_K \sqrt{1-y_k^2}\, x_k^n e^{-\left(\gamma_{th}N_0/\phi P\lambda_y x_k\right)}, \quad (21)$$

where $x_k = (1/2)y_k(x_1 - (\gamma_{\text{th}}N_0/P(1-\delta))) + (1/2)(x_1 + (\gamma_{\text{th}}N_0/P(1-\delta)))$, $y_k = \cos(((2k-1)/2K)\pi)$, $\omega_K = \pi/K$ with K is a parameter that determines the tradeoff between complexity and accuracy.

Applying a similar method for I_3, we obtain an approximate expression of the SOP in the following corollary.

Corollary 4. *The approximate expression of the SOP is given by*

$$SOP = 1 - \exp\left(-\frac{\gamma_{th}N_0}{P(1-\delta)}\left(\frac{1}{\lambda_x} + \frac{1}{\lambda_y}\right)\right) when \frac{P < 2\phi\gamma_{th}N_0}{(1-\delta)^2}, \quad (22)$$

$$\begin{aligned} SOP \approx {} & 1 - e^{-\left((1/\lambda_x)+(1/\lambda_y)\right)\sqrt{\gamma_{th}N_0/2P\phi}} \\ & - \frac{1}{2}\sum_{n=0}^{N} \boxtimes \frac{(-1)^n}{n!}\left(\frac{1}{\lambda_x} - \frac{1}{\lambda_y}\right)^n \left(x_1 - \frac{\gamma_{th}N_0}{P(1-\delta)}\right)\sum_{k=1}^{K} \boxtimes \omega_K \sqrt{1-y_k^2}\, x_i^n \\ & \cdot \left(\frac{1}{\lambda_x} e^{-\left(\gamma_{th}N_0/\phi P\lambda_y x_k\right)} + \frac{1}{\lambda_y} e^{-\left(\gamma_{th}N_0/\phi P\lambda_x x_k\right)}\right) when \frac{P > 2\phi\gamma_{th}N_0}{(1-\delta)^2}. \end{aligned} \quad (23)$$

It is noted that higher K results in a smaller difference in the approximate SOP expression. However, the value of K cannot be arbitrarily large because of the computational complexity. Fortunately, for our considered system model, even a small value of K ensures that the approximate expression well fits the exact expression, as demonstrated in the next section.

Remark 5. In this paper, the two-way relay system with one relay node is considered. In the case of a two-way multiple relay system, we must first model the relay selection scheme mathematically to find the outage probability (OP) expression. Then, the OP expression will contain the components representing the relay selection algorithm. In the case of a two-way relay system where the relay is equipped with multiple antennas, the channels between the relay and two terminals are random matrices. Furthermore, in the third phase time, the relay may employ a beamforming or transmit antenna selection (TAS) technique to transmit its signals. Thus, the OP expression will contain the components representing the beamforming vector at the relay or TAS algorithm. To sum up, it is challenging to find the OP expressions in these two scenarios.

4. Numerical Results

In this section, we use the exact and approximation expressions of the UOP and SOP obtained in the previous section to evaluate the two-way DF system's outage performance with the EH relay. Various scenarios are carried out to reveal

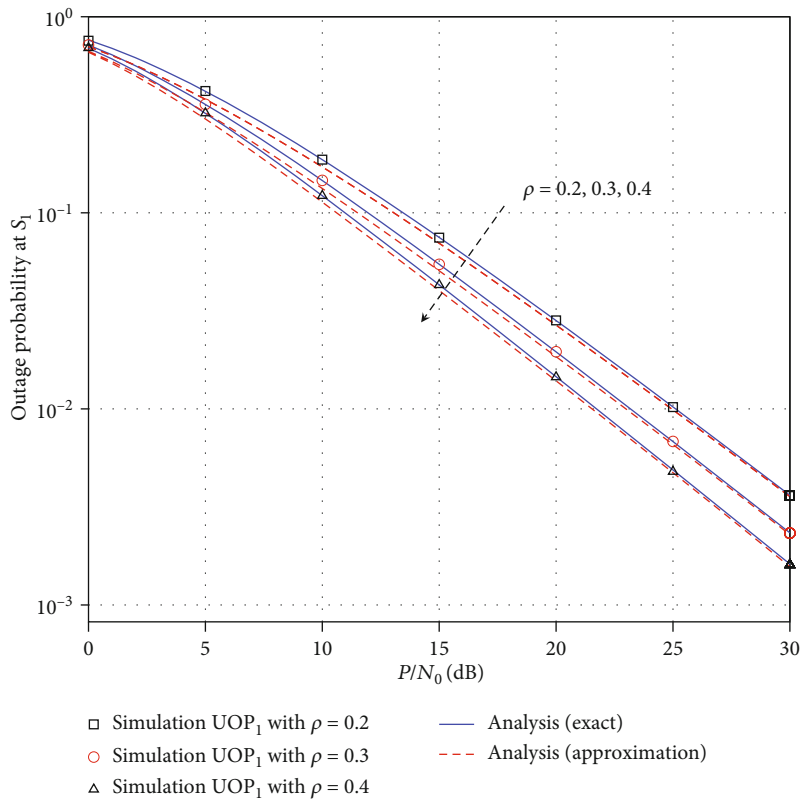

Figure 2: UOP of S_1 versus average SNRs for $\beta = 3$, $\gamma_{th} = 7$, $\eta = 0.8$, $\delta = 0.6$, $N_0 = 1$, $N = 5$, and $L = 5$.

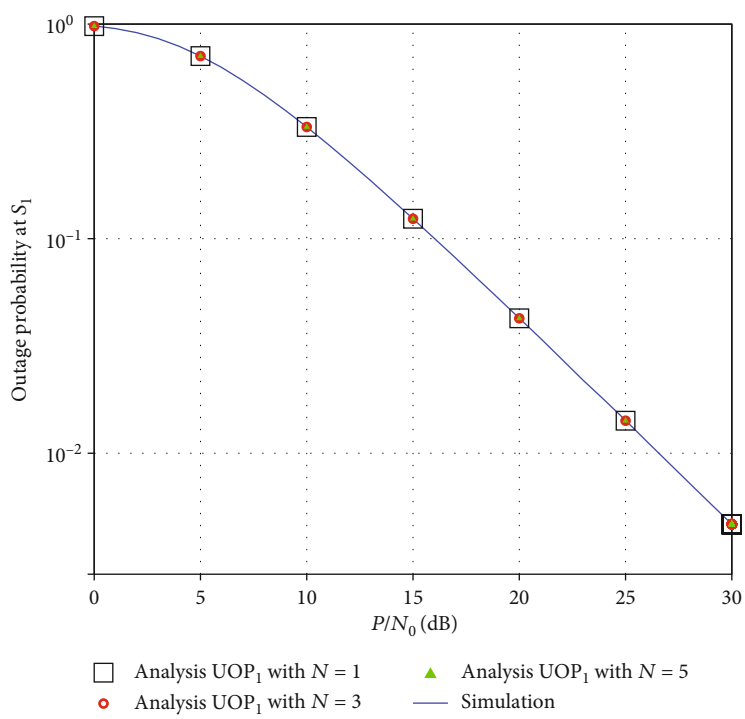

Figure 3: Effect of N on the UOP of S_1 for $\beta = 3$, $\gamma_{th} = 7$, $\eta = 0.8$, $\rho = 0.3$, $N_0 = 1$, and $L = 5$.

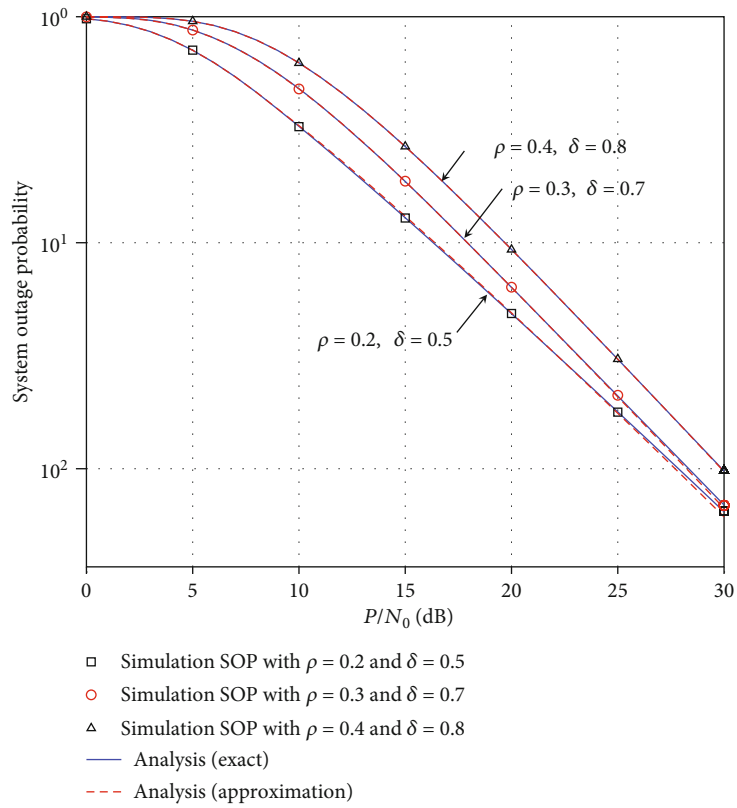

Figure 4: System outage probability versus average SNR for $\beta = 3$, $\gamma_{\text{th}} = 7$, $\eta = 0.8$, $N_0 = 1$, and $N = K = 5$.

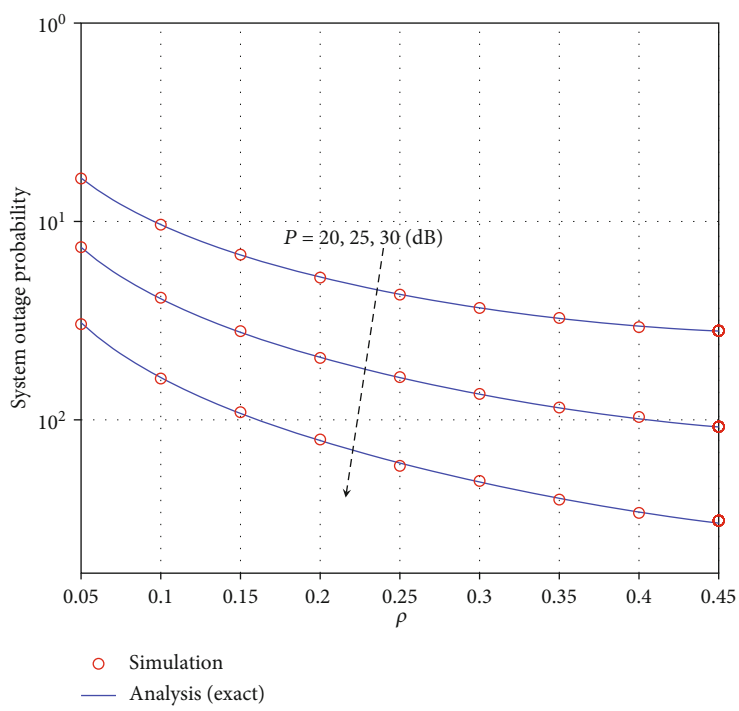

Figure 5: Effect of ρ on the system outage probability for different transmission power. $\beta = 3$, $\gamma_{\text{th}} = 7$, $\delta = 0.3$, $\eta = 0.8$, $N_0 = 1$, and $N = K = 5$.

the impact of the Rayleigh fading, users' transmission power, the time allocation ratio, and the power allocation coefficient on the system performance. To demonstrate the accuracy of the analysis results, we compare them with the Monte-Carlo simulation results. With regard to the simulation methodology, we first create the channel coefficients h_1 and

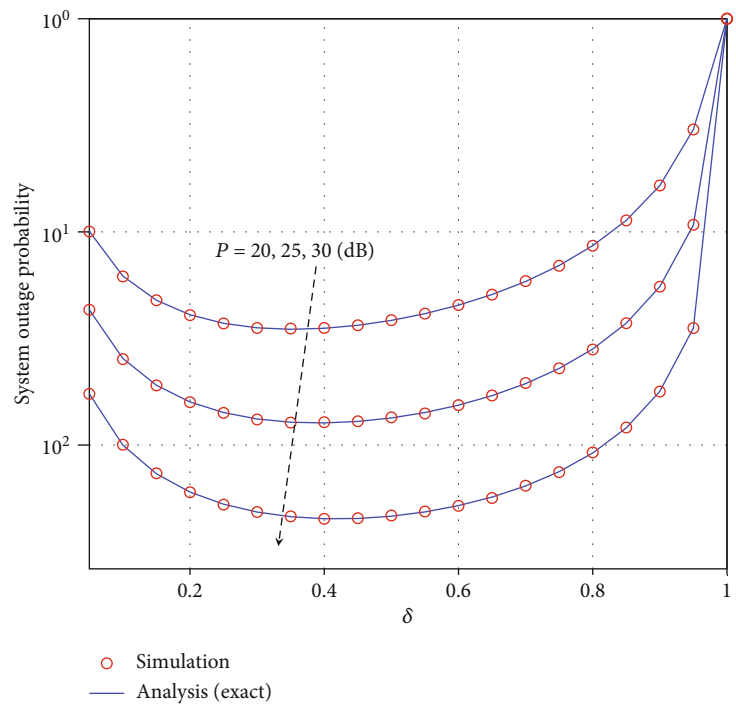

FIGURE 6: Effect of δ on the system outage probability for different transmission power. $\beta = 3$, $\gamma_{\text{th}} = 7$, $\eta = 0.8$, $\rho = 0.3$, $N_0 = 1$, and $N = K = 5$.

h_2 which are random variables with Rayleigh distribution with mean λ_x and λ_x, respectively. Then, we compute the SNR at the receivers. If this SNR is less than the predetermined threshold γ_{th}, then the outage happens. Such a process is repeated for a number of iterations of 10^6. The outage probability is determined as the ratio of the number of times the outage events occur to the number of samples. It is assumed that network nodes are located on a 2D plane. The distance between the two terminals S_1 and S_2 is normalized to 1. Specifically, the locations of all nodes are $S_1(0,0)$, $S_2(1,0)$, and $R(0.4,0)$. We denote d_1 and d_2 as the physical distances from R to S_1 and from R to S_2, respectively. For free-space path-loss transmission, we have $\lambda_x = d_1^{-\beta}$ and $\lambda_y = d_2^{-\beta}$, where β, $2 \le \beta \le 6$, is the path loss exponent. Unless otherwise stated, we set the following parameters $\beta = 3$, $\gamma_{\text{th}} = 7$, $\eta = 0.8$, $\delta = 0.6$, $N_0 = 1$, $N = 5$, and $K = L = 5$.

Figure 2 plots the exact and approximate analysis results and simulation results of the UOP of S_1 versus the average SNR P/N_0 for $\rho = 0.2$, 0.3, and 0.4. We can see that the analysis results are in excellent agreement with the simulation ones, proving the correctness of the derived mathematical expressions. Moreover, the approximate results obtained by using the Gaussian-Chebyshev quadrature approach as in (15) are very close to the exact results. In addition, we observe that as ρ increases, the UOP of S_1 is reduced. It is because the increased ρ makes the transmission power in the third phase higher, thus improving the probability of successfully decoding signal at S_1.

All theoretical analyses in this paper are based on the Taylor approximation method for exponential function such as in (A.4). For this approximation method, the accurateness can be enhanced by using more terms in the Taylor series. However, it may affect the computation time. To study the accurateness matter, we conduct an evaluation of the UOP of S_1 for a different number of terms in Taylor series expansion, i.e., $N = 1$, $N = 3$, and $N = 5$, and give the results in Figure 3. We can see that a small number of terms in Taylor series expansion can provide a good match between the analysis results and simulation results. Particularly, even when $N = 1$, the analysis results are very similar to the simulation results. It means that Taylor series expansion is an efficient approximation method in this paper.

Figure 4 presents the system outage probability versus the average SNR for three cases: (1) $\rho = 0.2, \delta = 0.5$; (2) $\rho = 0.3$, $\delta = 0.7$; and (3) $\rho = 0.4, \delta = 0.8$. It can be seen from Figure 4 that the simulation results and analysis results are coincident, confirming the correctness of the analysis steps in this paper. We can observe that when increasing ρ and δ, the SOP decreases. It is because as ρ and δ gets higher, the harvested energy of R in two phases increases. Consequently, its transmission power in the third phase increases, resulting in higher SNR.

Figure 5 shows the SOP versus the time allocation ratio of signal phase ρ for three cases of the transmission power, i.e., $P = 20$, 25, and 30 dB. As observed in Figure 5, as ρ increases, the SOP decreases, indicating that the communication quality between S_1 and S_2 is better.

To further investigate the influence of the power-splitting ratio δ on the system performance, we evaluate the SOP as δ ranges from 0 to 1 and depict the result in Figure 6. We can see that based on the derived mathematical expression, the optimal δ at which the system outage probability is smallest can be determined. Specifically, the optimal value of δ in Figure 6 corresponding to $P = 20$ dB, $P = 25$ dB, and $P = 30$ dB are 0.34, 0.4, and 0.45, respectively.

5. Conclusion

In this paper, we have derived the exact and approximate closed-form expressions of the user outage probability and the system outage probability of a two-way DF relay system where the relay is not powered by a separated power supply but harvests the energy from the received radio frequency signals in two phases to convert it into the transmission power in the third phase. The approximate expressions of these two kinds of outage probabilities are in explicit and simplified forms, providing a better understanding of the effects of parameters on the quality of the system. Moreover, the accuracy of the approximate expressions can be adjusted by changing the number of terms in Taylor series expansion and the coefficients in the Gaussian-Chebyshev quadrature approach. All analysis results are verified by Monte-Carlo simulation results. Numerical results show that when the time allocation of signal phase ρ increases, the system outage probability decreases. Furthermore, using numerical results can determine the optimal power-splitting ratio δ at which the system outage probability is smallest. The exact and approximate closed-form expressions of the UOP and SOP in this paper provide a solid foundation for analyzing the performance of two-way relay systems with EH relay under other performance metrics such as ergodic capacity, energy efficiency, and average symbol error probability.

Appendix

A. Proof of Theorem 1

To support the derivation of the closed-form expression of UOP, we present two functions $y_1 = \gamma_{\text{th}} N_0 / P(1-\delta)$ and $y_2 = (\gamma_{\text{th}} N_0 / \phi P x) - x$ in the Oxy coordinate plane to determine the integral domain as illustrated in Figure 7, where x_0 is the root of the equation $y_1 = y_2$.

Then, the UOP of S_1 can be calculated as

$$\text{UOP}_i = 1 - \underbrace{\int_0^{x_0} \int_{(\gamma_{th} N_0/\phi P x)-x}^{\infty} f_{XY}(x,y)\,dy\,dx}_{I_{1a}} - \underbrace{\int_{x_0}^{\infty} \int_{(\gamma_{th} N_0/P(1-\delta))}^{\infty} f_{XY}(x,y)\,dy\,dx}_{I_{1b}}, \tag{A.1}$$

where $f_{X,Y}(x,y)$ is the joint probability density function of two random variables X and Y, i.e.,

$$f_{XY}(x,y) = \frac{1}{\lambda_x} e^{-(x/\lambda_x)} \frac{1}{\lambda_y} e^{-(y/\lambda_y)}. \tag{A.2}$$

First, I_{1a} can be computed as

$$\begin{aligned} I_{1a} &= \int_0^{x_0} \int_{(\gamma_{th} N_0/\phi P x)-x}^{\infty} \frac{1}{\lambda_x \lambda_y} e^{-\left((x/\lambda_x)+(y/\lambda_y)\right)}\,dy\,dx \\ &= \frac{1}{\lambda_x} \int_0^{x_0} e^{-\left((1/\lambda_x)-(1/\lambda_y)\right)x - \left(\gamma_{th} N_0/\phi P \lambda_y x\right)}\,dx. \end{aligned} \tag{A.3}$$

Applying Taylor series expansion for $e^{-((1/\lambda_x)-(1/\lambda_y))x}$, i.e.,

$$e^{-\left((1/\lambda_x)-(1/\lambda_y)\right)x} = \sum_{n=0}^{\infty} \frac{(-1)^n}{n!} \left(\frac{1}{\lambda_x} - \frac{1}{\lambda_y}\right)^n x^n, \tag{A.4}$$

we have

$$I_{1a} = \frac{1}{\lambda_x} \sum_{n=0}^{N} \frac{(-1)^n}{n!} \left(\frac{1}{\lambda_x} - \frac{1}{\lambda_y}\right)^n \int_0^{x_0} x^n e^{-(\gamma_{th} N_0/\phi P \lambda_x x)}\,dx, \tag{A.5}$$

where N is the number of truncated terms in the series expansion.

With the help of [6] (Eq. (3.471.2)), we obtain

$$\begin{aligned} I_{1a} &= \frac{1}{\lambda_x} \sum_{n=0}^{N} \frac{(-1)^n}{n!} \left(\frac{1}{\lambda_x} - \frac{1}{\lambda_y}\right)^n \left(\frac{\gamma_{\text{th}} N_0}{\phi P \lambda_y}\right)^{n/2} \\ &\quad \times x_0^{(n+2)/2} e^{-\left(\gamma_{\text{th}} N_0/2\phi P \lambda_y x_0\right)} W_{(-n-2)/2,(n+1)/2}\left(\frac{\gamma_{\text{th}} N_0}{\phi P \lambda_y x_0}\right). \end{aligned} \tag{A.6}$$

Next, I_{1b} can be computed as

$$\begin{aligned} I_{1b} &= \int_{x_0}^{\infty} \int_{\gamma_{\text{th}} N_0/P(1-\delta)}^{\infty} \frac{1}{\lambda_x \lambda_y} e^{-\left((x/\lambda_x)+(y/\lambda_y)\right)}\,dy\,dx \\ &= \int_{x_0}^{\infty} \frac{1}{\lambda_x} e^{-(x/\lambda_x)} \left(\int_{\gamma_{\text{th}} N_0/P(1-\delta)}^{\infty} \frac{1}{\lambda_y} e^{-(y/\lambda_y)}\,dy\right) dx \\ &= e^{-\left((x_0/\lambda_x)+\left(\gamma_{\text{th}} N_0/P(1-\delta)\lambda_y\right)\right)}. \end{aligned} \tag{A.7}$$

Plugging (A.6) and (A.7) into (A.1), we get the closed-form expression of the UOP of S_1 as in (12).

B. Proof of Theorem 3

First, we find a closed-form expression of I_2. Substituting (6), (7), and (8) into (17), we have

$$\begin{aligned} I_2 &= \Pr\left(\begin{array}{c} X > \dfrac{\gamma_{\text{th}} N_0}{P(1-\delta)}, Y > \dfrac{\gamma_{\text{th}} N_0}{P(1-\delta)}, \\ (X+Y)X > \dfrac{\gamma_{\text{th}} N_0}{\phi P}, Y > X \end{array}\right) \\ &= \Pr\left(X > \frac{\gamma_{\text{th}} N_0}{P(1-\delta)}, (X+Y)X > \frac{\gamma_{\text{th}} N_0}{\phi P}, Y > X\right) \\ &= \Pr\left(X > \frac{\gamma_{\text{th}} N_0}{P(1-\delta)}, Y > \frac{\gamma_{\text{th}} N_0}{\phi P X} - X, Y > X\right). \end{aligned} \tag{B.1}$$

B.1. Case 1: The Transmission Power $P < 2\phi\gamma_{th} N_0/(1-\delta)^2$. Considering the case when two terminals have transmission power satisfying the condition $P < 2\phi\gamma_{\text{th}} N_0/(1-\delta)^2$, the

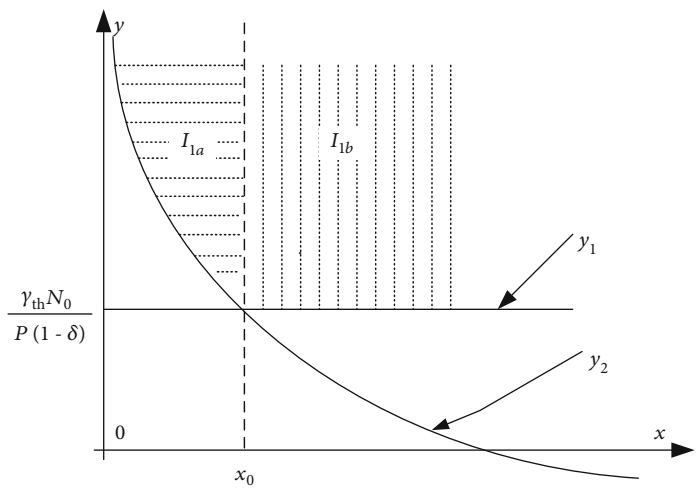

Figure 7: The integral calculation domain for I_{1a} and I_{1b}.

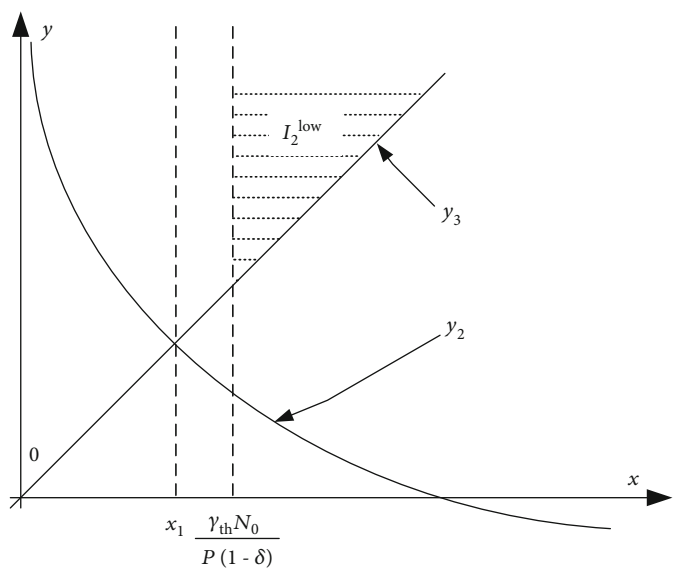

Figure 8: The integral calculation domain for I_2 in the low power region.

integral domain for I_2 in the low power region, I_2^{low}, is presented in Figure 8, where $y_2 = (\gamma_{\text{th}}N_0/\phi Px) - x$ and $y_3 = x$, and x_1 is the root of the equation $y_2 = y_3$.

Based on Figure 8, we have

$$I_2^{\text{low}} = \int_{\gamma_{\text{th}}N_0/P(1-\delta)}^{\infty} \int_{x}^{\infty} f_{X,Y}(x,y)\, dydx, \tag{B.2}$$

where $f_{X,Y}(x,y)$ is the joint probability density function of two random variables X and Y given in (A.2).

Substituting (A.2) into (B.2), we can calculate I_2^{low} as

$$I_2^{\text{low}} = \frac{\lambda_y}{\lambda_x + \lambda_y} \exp\left(-\frac{\gamma_{\text{th}}N_0}{P(1-\delta)}\left(\frac{1}{\lambda_x} + \frac{1}{\lambda_y}\right)\right). \tag{B.3}$$

Similarly, we can also calculate I_3 in the low transmission power region, I_3^{low}, as

$$I_3^{\text{low}} = \frac{\lambda_x}{\lambda_x + \lambda_y} \exp\left(-\frac{\gamma_{\text{th}}N_0}{P(1-\delta)}\left(\frac{1}{\lambda_x} + \frac{1}{\lambda_y}\right)\right). \tag{B.4}$$

Plugging (B.3) and (B.2) into (16), we obtain the SOP in the low SNR region as in (19).

B.2. Case 2: The Transmission Power $P > 2\phi\gamma_{th}N_0/(1-\delta)^2$. Considering the case when two terminals have transmission power satisfying the condition $P > 2\phi\gamma_{\text{th}}N_0/(1-\delta)^2$, from (B1), we split the integral domain of I_2 in the high SNR region into two small regions I_{2a} and I_{2b} as in Figure 9.

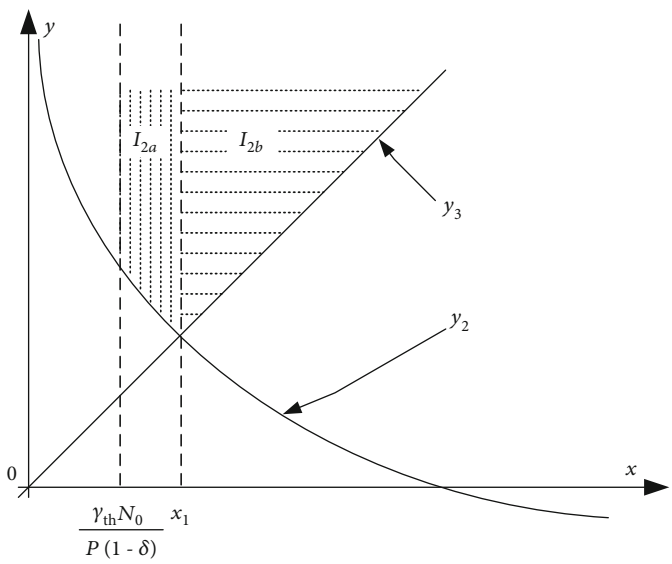

Figure 9: The integral calculation domain for I_2 in the high power region.

Based on Figure 9, I_2 can be computed as

$$I_2 = \underbrace{\int_{\gamma_{\text{th}}N_0/P(1-\delta)}^{x_1} \int_{(\gamma_{\text{th}}N_0/P\phi x)-x}^{\infty} f_{XY}(x,y)\,dy\,dx}_{I_{2a}} + \underbrace{\int_{x_1}^{\infty}\int_{x}^{\infty} f_{XY}(x,y)\,dy\,dx}_{I_{2b}}. \tag{B.5}$$

The first part of (B.5), I_{2a}, can be calculated as

$$\begin{aligned} I_{2a} &= \int_{\gamma_{\text{th}}N_0/P(1-\delta)}^{x_1} \int_{(\gamma_{\text{th}}N_0/P\phi x)-x}^{\infty} \frac{1}{\lambda_x\lambda_y} e^{-(x/\lambda_x)-(y/\lambda_y)}\,dy\,dx \\ &= \int_{\gamma_{\text{th}}N_0/P(1-\delta)}^{x_1} \frac{1}{\lambda_x} e^{-(x/\lambda_x)} e^{-(1/\lambda_y)((\gamma_{\text{th}}N_0/P\phi x)-x)}\,dx \\ &= \frac{1}{\lambda_x}\int_{\gamma_{\text{th}}N_0/P(1-\delta)}^{x_1} e^{-x\left((1/\lambda_x)-(1/\lambda_y)\right)-\left(\gamma_{\text{th}}N_0/\lambda_y P\phi x\right)}\,dx. \end{aligned} \tag{B.6}$$

Recalling the Taylor series expansion in (A.4), we can rewrite (B.6) as

$$\begin{aligned} I_{2a} &= \frac{1}{\lambda_x}\sum_{n=0}^{N} \frac{(-1)^n}{n!}\left(\frac{1}{\lambda_x}-\frac{1}{\lambda_y}\right)^n \int_{\gamma_{\text{th}}N_0/P(1-\delta)}^{x_1} x^n e^{-\left(\gamma_{\text{th}}N_0/\phi P\lambda_y x\right)}\,dx \\ &= \frac{1}{\lambda_x}\sum_{n=0}^{N} \frac{(-1)^n}{n!}\left(\frac{1}{\lambda_x}-\frac{1}{\lambda_y}\right)^n \int_{0}^{x_1} x^n e^{-\left(\gamma_{\text{th}}N_0/\phi P\lambda_y x\right)}\,dx \\ &\quad - \frac{1}{\lambda_x}\sum_{n=0}^{N} \frac{(-1)^n}{n!}\left(\frac{1}{\lambda_x}-\frac{1}{\lambda_y}\right)^n \int_{0}^{\gamma_{\text{th}}N_0/P(1-\delta)} x^n e^{-\left(\gamma_{\text{th}}N_0/\phi P\lambda_y x\right)}\,dx. \end{aligned} \tag{B.7}$$

Applying [27] (Eq. (3.471.2)), we obtain

$$\begin{aligned} I_{2a} &= \frac{1}{\lambda_x}\sum_{n=0}^{N} \frac{(-1)^n}{n!}\left(\frac{1}{\lambda_x}-\frac{1}{\lambda_y}\right)^n \left(\frac{\gamma_{\text{th}}N_0}{\phi P\lambda_y}\right)^{n/2} \\ &\quad \cdot \left(\begin{array}{l} x_1^{(n+2)/2} e^{-\left(\gamma_{\text{th}}N_0/2\lambda_y\phi P x_1\right)} W_{(-n-2)/2,(n+1)/2}\left(\dfrac{\gamma_{\text{th}}N_0}{\lambda_y\phi P x_1}\right) \\ -\left(\dfrac{\gamma_{\text{th}}N_0}{P(1-\delta)}\right)^{(n+2)/2} e^{-\frac{(1-\delta)}{2\lambda_y\phi}} W_{(-n-2)/2,(n+1)/2}\left(\dfrac{(1-\delta)}{\lambda_y\phi}\right) \end{array} \right). \end{aligned} \tag{B.8}$$

The second part of (B.5), I_{2b}, can be calculated as

$$\begin{aligned} I_{2b} &= \int_{x_1}^{\infty}\int_{x}^{\infty} f_{XY}(x,y)\,dy\,dx = \int_{x_1}^{\infty}\int_{x}^{\infty} \frac{1}{\lambda_x\lambda_y} e^{-(x/\lambda_x)-(y/\lambda_y)}\,dy\,dx \\ &= \frac{1}{\lambda_x}\int_{x_1}^{\infty} e^{-x\left((1/\lambda_x)+(1/\lambda_y)\right)}\,dx = \frac{\lambda_y}{\lambda_x+\lambda_y} e^{-\left((1/\lambda_x)+(1/\lambda_y)\right)\sqrt{\gamma_{\text{th}}N_0/2\phi P}}. \end{aligned} \tag{B.9}$$

Substituting (B.8) and (B.9) into (B.5), I_2 finally becomes

$$\begin{aligned} I_2 &= \frac{\lambda_y}{\lambda_x+\lambda_y} e^{-\left((1/\lambda_x)+(1/\lambda_y)\right)\sqrt{\gamma_{\text{th}}N_0/2\phi P}} \\ &\quad + \frac{1}{\lambda_x}\sum_{n=0}^{N} \frac{(-1)^n}{n!}\left(\frac{1}{\lambda_x}-\frac{1}{\lambda_y}\right)^n \left(\frac{\gamma_{\text{th}}N_0}{\phi P\lambda_y}\right)^{n/2} \\ &\quad \cdot \left(\begin{array}{l} x_1^{(n+2)/2} e^{-\left(\gamma_{\text{th}}N_0/2\lambda_y\phi P x_1\right)} W_{(-n-2)/2,(n+1)/2}\left(\dfrac{\gamma_{\text{th}}N_0}{\lambda_y\phi P x_1}\right) \\ -\left(\dfrac{\gamma_{\text{th}}N_0}{P(1-\delta)}\right)^{(n+2)/2} e^{-(1-\delta)/2\lambda_y\phi} W_{(-n-2)/2,(n+1)/2}\left(\dfrac{(1-\delta)}{\lambda_y\phi}\right) \end{array} \right). \end{aligned} \tag{B.10}$$

By using the above analysis steps for I_3, the closed-form expression of I_3 is given by

$$I_3 = \frac{\lambda_x}{\lambda_y + \lambda_x} e^{-\left(\left(1/\lambda_y\right)+\left(1/\lambda_x\right)\right)\sqrt{\gamma_{\text{th}} N_0/2\phi P}} + \frac{1}{\lambda_y}\sum_{n=0}^{N} \boxtimes \frac{(-1)^n}{n!}\left(\frac{1}{\lambda_y} - \frac{1}{\lambda_x}\right)^n \left(\frac{\gamma_{\text{th}} N_0}{\phi P \lambda_x}\right)^{n/2} \cdot \left(\begin{array}{c} x_1^{(n+2)/2} e^{-(\gamma_{\text{th}} N_0/2\lambda_x \phi P x_1)} W_{(-n-2)/2,(n+1)/2}\left(\frac{\gamma_{\text{th}} N_0}{\lambda_x \phi P x_1}\right) \\ -\left(\frac{\gamma_{\text{th}} N_0}{P(1-\delta)}\right)^{(n+2)/2} e^{-((1-\delta)/(2\lambda_x \phi))} W_{(-n-2)/2,(n+1)/2}\left(\frac{1-\delta}{\lambda_x \phi}\right) \end{array} \right). \tag{B.11}$$

Then, substituting (B.10) and (B.11) into (16), we obtain the closed-form expression of the SOP in the high SNR region as in (20).

Data Availability

Data are available on request.

Conflicts of Interest

The authors declare that they have no conflicts of interest.

References

[1] A. A. Nasir, X. Zhou, S. Durrani, and R. A. Kennedy, "Relaying protocols for wireless energy harvesting and information processing," *IEEE Transactions on Wireless Communications*, vol. 12, no. 7, pp. 3622–3636, 2013.

[2] N. Zlatanov, R. Schober, and Z. Hadzi-Velkov, "Asymptotically optimal power allocation for energy harvesting communication networks," *IEEE Transactions on Vehicular Technology*, vol. 99, pp. 1–1, 2017.

[3] V. D. Nguyen, T. Q. Duong, H. D. Tuan, O. S. Shin, and H. V. Poor, "Spectral and energy efficiencies in full-duplex wireless information and power transfer," *IEEE Transactions on Communications*, vol. 65, no. 5, pp. 2220–2233, 2017.

[4] K. Tutuncuoglu, B. Varan, and A. Yener, "Optimum transmission policies for energy harvesting two-way relay channels," in *2013 IEEE International Conference on Communications Workshops (ICC)*, pp. 586–590, Budapest, Hungary, 2013.

[5] D. Wang, R. Zhang, X. Cheng, L. Yang, and C. Chen, "Relay selection in full-duplex energy-harvesting two-way relay networks," *IEEE Transactions on Green Communications and Networking*, vol. 1, no. 2, pp. 182–191, 2017.

[6] H. Cao, L. Fu, and H. Dai, "Throughput analysis of the two-way relay system with network coding and energy harvesting," in *2017 IEEE International Conference on Communications (ICC)*, pp. 1–6, Paris, France, 2017.

[7] L. R. Varshney, "Transporting information and energy simultaneously," in *2008 IEEE International Symposium on Information Theory*, pp. 1612–1616, Toronto, ON, Canada, 2008.

[8] L. Liu, R. Zhang, and K. C. Chua, "Wireless information and power transfer: a dynamic power splitting approach," *IEEE Transactions on Communications*, vol. 61, no. 9, pp. 3990–4001, 2013.

[9] X. Zhou, R. Zhang, and C. K. Ho, "Wireless information and power transfer: architecture design and rate-energy tradeoff," *IEEE Transactions on Communications*, vol. 61, no. 11, pp. 4754–4767, 2013.

[10] I. Krikidis, Z. Gan, and B. Ottersten, "Harvest-use cooperative networks with half/full-duplex relaying," in *2013 IEEE Wireless Communications and Networking Conference (WCNC)*, pp. 4256–4260, Shanghai, China, 2013.

[11] Y. Gu and S. Aissa, "RF-based energy harvesting in decode-and-forward relaying systems: ergodic and outage capacities," *IEEE Transactions on Wireless Communications*, vol. 14, no. 11, pp. 6425–6434, 2015.

[12] B. Medepally and N. B. Mehta, "Voluntary energy harvesting relays and selection in cooperative wireless networks," *IEEE Transactions on Wireless Communications*, vol. 9, no. 11, pp. 3543–3553, 2010.

[13] L. Liu, R. Zhang, and K.-C. Chua, "Wireless information transfer with opportunistic energy harvesting," *IEEE Transactions on Wireless Communications*, vol. 12, no. 1, pp. 288–300, 2012.

[14] R. Boris and W. Armin, "Spectral efficient protocols for half-duplex fading relay channels," *IEEE Journal on Selected Areas in Communications*, vol. 25, no. 2, pp. 379–389, 2007.

[15] V. N. Q. Bao, H. Van Toan, and K. N. Le, "Performance of two-way AF relaying with energy harvesting over Nakagami-*m* fading channels," *IET Communications*, vol. 12, no. 20, pp. 2592–2599, 2018.

[16] S. Atapattu, J. Yindi, J. Hai, and C. Tellambura, "Relay selection schemes and performance analysis approximations for two-way networks," *IEEE Transactions on Communications*, vol. 61, no. 3, pp. 987–998, 2013.

[17] K. Hwang, M. Ju, and M. Alouini, "Outage performance of opportunistic two-way amplify-and-forward relaying with outdated channel state information," *IEEE Transactions on Communications*, vol. 61, no. 9, pp. 3635–3643, 2013.

[18] D. K. Nguyen, M. Matthaiou, T. Q. Duong, and H. Ochi, "RF energy harvesting two-way cognitive DF relaying with transceiver impairments," in *2015 IEEE International Conference on Communication Workshop (ICCW)*, pp. 1970–1975, London, UK, 2015.

[19] K. Tutuncuoglu, B. Varan, and A. Yener, "Throughput maximization for two-way relay channels with energy harvesting nodes: the impact of relaying strategies," *IEEE Transactions on Communications*, vol. 63, no. 6, pp. 2081–2093, 2015.

[20] W. Li, M.-L. Ku, Y. Chen, K. R. Liu, and S. Zhu, "Performance analysis for two-way network-coded dual-relay networks with stochastic energy harvesting," *IEEE Transactions on Wireless Communications*, vol. 16, no. 9, pp. 5747–5761, 2017.

[21] N. T. P. Van, S. F. Hasan, X. Gui, S. Mukhopadhyay, and H. Tran, "Three-step two-way decode and forward relay with energy harvesting," *IEEE Communications Letters*, vol. 21, no. 4, pp. 857–860, 2017.

[22] L. Shi, Y. Ye, R. Q. Hu, and H. Zhang, "System outage performance for three-step two-way energy harvesting DF relaying," *IEEE Transactions on Vehicular Technology*, vol. 68, no. 4, pp. 3600–3612, 2019.

[23] H. Liang, C. Zhong, H. Lin, Y. Li, and Z. Zhang, "Optimization and analysis of wireless powered multi-antenna two-way relaying systems," *IEEE Transactions on Communications*, vol. 68, no. 4, pp. 2048–2060, 2020.

[24] C. Zhang and X. Jia, "Joint beamforming optimisation for NOMA-based wireless powered multi-pair two-way AF and

DF relaying networks," *IET Communications*, vol. 13, no. 4, pp. 387–395, 2019.

[25] P. Ramezani and A. Jamalipour, "Two-way dual-hop WPCN with a practical energy harvesting model," *IEEE Transactions on Vehicular Technology*, vol. 69, no. 7, pp. 8013–8017, 2020.

[26] A. Bletsas, A. Khisti, D. P. Reed, and A. Lippman, "A simple cooperative diversity method based on network path selection," *IEEE Journal on Selected Areas in Communications*, vol. 24, no. 3, pp. 659–672, 2006.

[27] I. S. Gradshteyn, I. M. Ryzhik, A. Jeffrey, and D. Zwillinger, *Table of Integrals, Series and Products, 7th ed. Amsterdam*, Elsevier, Boston, 2007.